Assessing skin hydration status in haemodialysis patients using terahertz spectroscopy: a pilot/feasibility study

Filip Kadlec[1]**, Milan Berta**[1]**, Petr Kužel**[1]**, František Lopot**[2]
and Vladimír Polakovič[2]

[1] Institute of Physics, Academy of Sciences of the Czech Republic, Na Slovance 2,
182 21 Prague 8, Czech Republic
[2] Department of Medicine, General University Hospital, Šermířská 5, 169 00 Prague 6,
Czech Republic

E-mail: kadlecf@fzu.cz

Abstract
Terahertz (THz) time-domain spectroscopy was used *in vivo* to measure the
body reflectance with the aim of determining experimentally the influence of
haemodialysis on the content of water in the human skin. For this purpose,
an original methodology of determining the skin properties at THz frequencies
from the reflectance was developed. A series of measurements were performed
before and after dialysis with ten subjects. The results strongly indicate that
the surface body hydration is not the main parameter determining the skin
conductivity in the THz range.

(Some figures in this article are in colour only in the electronic version)

1. Introduction

Haemodialysis (HD) is one of the main methods of renal disease treatment applied on a regular
basis to nearly one million patients worldwide. During HD, potassium, urea, free water and
other waste metabolites are removed from the patient's blood, usually three times a week.
Determining the optimal amount of water to be removed is important in order to reduce both
short-term, i.e. intradialytic problems (cramps, hypotensions) as well as long-term adverse
effects of fluid dysbalance (hypervolemia-induced hypertension, accelerated loss of residual
renal function caused by repeated states of hypovolemia). Bioimpedance spectroscopy (BIS)
measurements can provide useful data (Matthie *et al* 1998); however, the evaluation of raw BIS
values is based on their subsequent transformation into volumes of different compartments
of body fluid. This procedure relies on a number of simplifying assumptions which may
substantially decrease the accuracy of the method (Kyle *et al* 2004). Consequently, up to
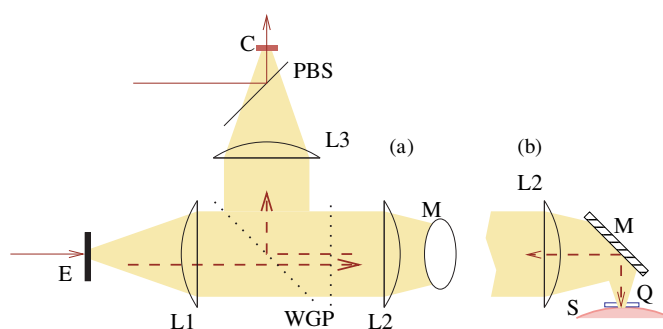
Figure 1. Schematics of the THz beam path in the experiment. (a) top view, (b) side view. E: THz wave emitter, L1–L3: lenses, WGP: wire grid polarizers, M: mirror, Q: quartz window, S: skin sample, PBS: pellicle beam splitter, C: electro-optic crystal (THz sensor). The thin solid lines with arrows represent the path of the laser pulses.

now, the amount of fluid to be removed during the HD process is strongly dependent on the physicians' experience. Therefore, developing new methods providing at least an estimation of the body hydration state appears as highly desirable.

Terahertz spectroscopy is one of the relatively recent experimental methods operating in the part of the electromagnetic spectrum often called 'terahertz gap'. This term refers to the fact that the relevant frequencies, of the order of 10^{12} Hz, could be accessed in the past neither by electronic methods from one side nor by optical ones from the other side of the spectrum. Fast development of the THz spectroscopy starting from the 1990s was triggered by the invention of a new class of lasers providing femtosecond pulses. Since then, great progress has been achieved, and the first applications, including those in medicine and biology, start to emerge; one of the most advanced ones concerns diagnosing skin cancer (Woodward 2002) and breast tumours (Fitzgerald *et al* 2006). The observed contrast between the diseased and healthy tissue has been attributed above all to the variable water content according to the skin condition. The pronounced interaction of the THz radiation with water makes it suitable for biomedical applications; at the same time, its wavelength of the order of a few hundreds of microns is another potential advantage for attaining a useful spatial resolution in imaging.

The present work has been motivated by the conjecture that, given the strong interaction between the THz radiation and the body water, it might be possible to determine the water content variations as a consequence of dialysis. Since the THz waves penetrate only a few hundreds of microns into the skin, the experiments were expected to reveal information about the water content in epidermis, while more deeply located parts of the body (in particular veins) remain out of reach of the THz radiation. The intracellular water content is supposed to remain approximately constant; therefore, the HD should manifest itself in reducing the extracellular water proportion. Since the mean size of cells is much smaller than the wavelength, the THz radiation is expected to be absorbed by both extracellular and intracellular water. Considering the well-known loss of skin turgor (Fayomi *et al* 2007, Mandal *et al* 1996, Vivanti *et al* 2007) induced by fluid removal during dialysis we speculated that even the low penetration depth of the THz radiation might provide information on hydration status of the patients in general.

2. Experimental details

A time-domain THz spectroscopy (TDTS) (Ferguson and Zhang 2002) experimental setup operating in reflection geometry under normal incidence (see figure 1) was used for measuring

the temporal waveforms of THz waves after interaction with the skin. Linearly polarized THz pulses were generated using femtosecond pulses provided by a Ti:sapphire laser (Coherent Vitesse) photoexciting a semiconductor-based large-area interdigitated emitter E (Dreyhaupt *et al* 2005). The emitter was biased with an ac voltage having a shape of rectangular pulses at a repetition rate of about 80 kHz. The THz beam was guided horizontally using two wire-grid polarizers WGP, three Picarin lenses L1–L3 and a skewed flat mirror M which turned the beam direction vertical in the sampling part of the setup. A 0.5 mm thick *c*-cut (0 0 0 1) quartz window Q with a circular clear aperture of 10 mm was fixed horizontally in the focal plane in order to enable a measurement with the skin S put in contact from below. The lateral width of the THz beam at the window did not exceed 3 mm for the low frequency part of the pulse spectrum (0.25 THz). The reflected THz beam was recombined linearly with a weak part of the laser beam with the aid of a thin pellicle beam splitter (PBS). The electro-optic sampling technique (Nahata *et al* 1999) with a 1 mm thick ⟨110⟩ ZnTe crystal C was used for the detection of the electric field intensity E as a function of time delay t.

The measurements were performed with ten volunteers, all of them stable HD patients with blood access provided by an arteriovenous fistula. The group included two women and eight men, all fair-skinned Caucasians, aged from 50 to 83 with the mean value of 63.5 years. Both TDTS (0.3–1.3 THz) and BIS measurements (Body Composition Monitor, Fresenius, operating in the frequency range 5 kHz–1 MHz) were performed prior to and after two HD sessions for each patient, one after a 3 days' and one after a 2 days' interdialytic interval. Besides, the patients' height, weight, age and ultrafiltrated fluid volumes were recorded. Three locations were chosen on the patients' non-access arms for the TDTS measurements. Two of them were located in the middle part of the volar forearm which had been indicated as convenient by previous studies (Pickwell *et al* 2004), and marked on the skin in order to permit us to repeat later measurements at the same spots. As the third placement, the tip of the ring-finger was chosen as a spot which can easily be located and where stratum corneum (SC) is expected to be relatively thin. A rapid-scan regime was applied in which acquiring one waveform takes approximately 10 s. Each THz waveform was acquired three times in order to avoid possible deviations of the data owing to small changes of contact between the window and measured skin; only if the differences between the three acquisitions were sufficiently small, the averaged curve was treated further, otherwise the measurement was repeated.

3. Data evaluation

In the experiments, time-domain waveforms $E(t)$ representing the electric field incident on the electro-optic crystal were recorded; an example is shown in figure 2. In the waveforms, two distinct peaks can easily be identified, each of them corresponding to a reflection at one interface. The peak (1) at $t = 0$ ps, due to the reflection at the (top) air–quartz interface, served as a reference, while the second peak around $t = 7$ ps, corresponding to the reflection at the bottom window surface in contact with the skin, was used for determining the THz properties of the skin. These results indicate that the refractive index value of the outermost layer of the skin, SC, is very close to that quartz, since there is no noticeable reflection from the quartz–SC interface. As we will show below, the presence of SC manifests itself by a time shift of the peak (2) only, the shape can therefore be attributed to the properties of epidermis. We do not observe a third peak at any later delay, which implies that the power penetrating to the epidermis–dermis interface is very low and the influence of dermis can be neglected.

The part of the waveforms at $t > 1$ ps contains supplementary small oscillations which are due to the presence of water vapour in the air. The relative air humidity varied between 20 and 30%, and, if uncorrected, it would have added a small error to the data evaluation,
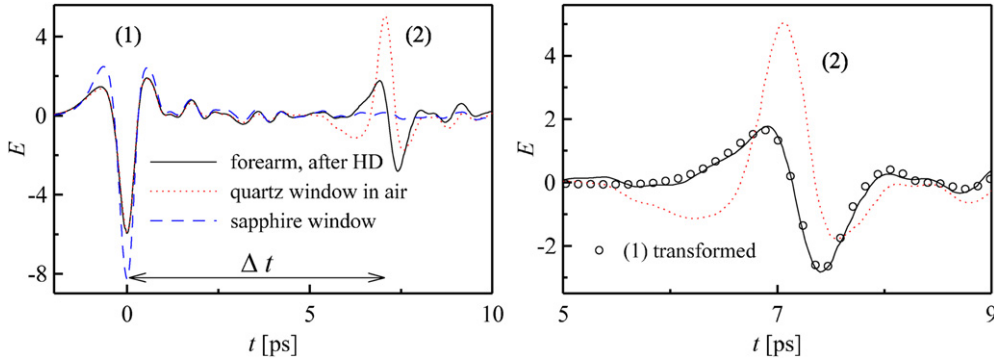
Figure 2. Example of waveforms measured to characterize the response of patient's skin at a selected location. Left: raw signal waveform $E(t)$ obtained on volar forearm (solid line), free standing quartz window used as a reference waveform (dotted line) and free standing sapphire window (dashed line). The useful signal coming from the upper window surface is located in the region marked as (1), the reflection from the lower surface in contact with the skin is located in the region (2). Right: a detailed view of the region (2). The solid and dashed lines correspond to the same data as in the left part. The open circles represent the peak (1) of the solid line, transformed according to the procedure described in the text.

since the oscillations extend also across the peak (2). In order to avoid this error, we made additional reference measurements for every particular day using a free-standing *c*-cut sapphire window with a higher optical thickness. The corresponding waveform (dashed line in figure 2) contains the same pattern of oscillations after the peak (1) proportional to its intensity; the peak (2) occurs at a later time ($t > 10$ ps, not shown in figure 2). Thus, it is possible to subtract the unwanted perturbation of the signal from the waveforms containing the information about skin samples.

The computation of reflectance spectra of the skin within the accessible spectral range has shown that its complex reflectance is essentially frequency-independent within the range from 0.3 to 1.3 THz which includes the majority of the transmitted THz power. In the lowest part of the spectra, below 0.3 THz, a steep increase in reflectance amplitude is observed systematically, but this part involves only a small portion of the THz power and it was subject to a higher level of experimental error. Therefore, as a good approximation, the THz properties of the epidermis can be reduced to one value of the complex refractive index. Below, we describe the way of obtaining this value from the raw experimental time-domain waveforms.

In our model, the matter involved in the interaction with THz radiation is represented by a sequence of four adjoining layers: air, quartz, SC and epidermis. These are separated by plane boundaries; their refractive indices are respectively 1, $n_q = 2.12$, n_{sc} and N_{ep}. As mentioned above, the experiment does not provide access to n_{sc}; we can merely roughly estimate the SC thickness if we presume that $n_{sc} = n_q$. Out of these layers, only epidermis is supposed to contain a significant amount of water, therefore only N_{ep} is assumed to have a non-zero imaginary part.

Denoting by E_0 the incident electric field, the reflectance of the air–quartz interface characterizing the pulse (1) in figure 2 is given by

$$r_1 = \frac{E_1}{E_0} = \frac{1 - n_q}{1 + n_q} \tag{1}$$

which is a real number. The reflectance coefficient describing the pulse (2) is complex and combines the reflectivity of the quartz (SC)–epidermis interface, the reflection losses at the

air–quartz interface and propagation through quartz and SC,

$$r_2 = \frac{E_2}{E_0} = \frac{n_q - N_{ep}}{n_q + N_{ep}} \frac{4n_q}{(1 + n_q)^2} \exp[2i\omega n_q (d_q + d_{SC})/c], \tag{2}$$

where ω is the THz probing frequency and d_q, d_{SC} are the quartz and SC thicknesses, respectively. In this formula, multiple reflections within the quartz window have been omitted because they are well separated in time. By dividing these two reflectances we eliminate the unknown E_0:

$$\tilde{r} = \frac{r_2}{r_1} = \frac{n_q - N_{ep}}{n_q + N_{ep}} \frac{4n_q}{1 - n_q^2} \exp[2i\omega n_q (d_q + d_{SC})/c]; \tag{3}$$

the experimental data are such that, within the experimental error, we can write

$$\tilde{r} = r \, e^{i(\phi + \omega \Delta t)}, \tag{4}$$

where r and ϕ are frequency-independent. The parameter Δt can be identified with the time delay due to propagation of waves through the quartz and SC described by the phase term in (3). The refractive index of epidermis can be expressed as

$$N_{ep} = n_q \frac{A - r \, e^{i\phi}}{A + r \, e^{i\phi}}, \qquad \text{where} \quad A = \frac{4n_q}{1 - n_q^2}. \tag{5}$$

The three free parameters, $\Delta t, r$ and ϕ, can easily be determined for each curve by transforming the first peak in the waveform so as to coincide with the second one. For this purpose, the relevant part of the $E(t)$ curve should be shifted by a time-delay Δt, scaled by a factor r and, finally, undergo a frequency-constant phase shift ϕ. In other words, the ratio of the Fourier transforms of the parts (1) and (2) of the signal waveforms $E_1(\omega)$, $E_2(\omega)$ should be equal to

$$\frac{E_2(\omega)}{E_1(\omega)} = \tilde{r} \, e^{i(\phi + \omega \Delta t)}. \tag{6}$$

Indeed, this behaviour is found in our spectra, which confirms the fact that within the most of our available frequency range, the complex refractive index of epidermis is almost constant. Hence, the coefficients $\Delta t, r$ and ϕ can easily be deduced from the experimental data. With a proper choice of the parameter values, the shape of the transformed peak (1) (shown by circles in figure 2) will be very close to that of the peak (2) (with oscillations due to water vapour subtracted). N_{ep} can then be obtained via (5). From the refractive index of epidermis, one can easily calculate the complex permittivity $\tilde{\varepsilon}_{ep} = N_{ep}^2$ or its complex conductivity $\tilde{\sigma}_{ep}$ which is related to its refractive index by

$$\tilde{\sigma}_{ep} = -i\omega\varepsilon_0 \tilde{\varepsilon}_{ep} \equiv -i\,\omega\varepsilon_0 N_{ep}^2, \tag{7}$$

where ε_0 denotes the vacuum permittivity. The complex quantities $N_{ep} = n_{ep} + i\kappa_{ep}$, $\tilde{\varepsilon}_{ep}$ and $\tilde{\sigma}_{ep}$ contain of course the same information as the pair of variables r, ϕ and they are just different representations of the properties of epidermis in the THz range. While the refractive index is an optical variable directly obtained from the experimental data and linked to the propagation of waves, the permittivity and conductivity are variables characterizing the physical response of the system. There is no agreement on the preferential use of these variables in the literature; consequently, for the sake of comparison with other results, it is often useful to consider more than one representation.

4. Results and discussion

Our data allow us to determine the interval between reflections with a precision of ± 0.01 ps. While the time delay between the pulses reflected from the two surfaces of an empty quartz window amounts to 7.06 ps, the values of Δt obtained with forearm skin measurements have an average value of 7.22 ps; there is no measurable difference between values obtained before and after HD. In the case of measurements on fingers, the mean value of Δt is 7.17 ps before HD and 7.19 ps after HD. Expressed in thickness under the assumption $n_{sc} = n_q = 2.12$, the SC layer would be on average 11 μm thick at forearms, in good agreement with the previously reported value of 10 μm (Pickwell *et al* 2004). Furthermore, in our model, the mean thickness of SC at fingertips is about 8 and 9 μm before and after HD, respectively. This increase does not correspond to a real change of SC thickness due to HD but, rather, it indicates that there is probably either a small increase of n_{sc} or a slight dehydration of the SC–epidermis transition region occurring as a consequence of HD. However, the extent of this change is close to the limit of our experimental resolution; moreover, it appears to be uncorrelated with the ultrafiltrated volume. Consequently, the pulse time delay Δt does not appear to have a practical use for determining the skin hydration state.

We have evaluated the correlation between values of ϕ and r measured at the mentioned locations of volar forearms ($\phi_{1,2}$, $r_{1,2}$) and fingertips (ϕ_3, r_3) in the set of patients either before or after HD. Examples of resulting relationships are: $\phi_3 = 0.439\phi_1 + 0.890$ in a pre-HD state where the value of the correlation coefficient is $R^2 = 0.249$ or $r_2 = 0.345r_1 + 0.311$ from post-HD data with $R^2 = 0.404$. While the correlations are quite high, the proportioning coefficient was always far from unity. This is evidence of different tissue properties in all three measuring locations and thus it suggests the need for some kind of standardization in the measurement site selection. The mutual correlations of HD-induced changes in ϕ and r measured at different locations were generally worse (R^2 reaching 0.15 or less). The weakest statistically insignificant correlations ($R^2 < 0.1$) were observed between the changes in ϕ, r and conventional markers of fluid status changes (BIS-measured overhydration and HD machine indicated ultrafiltration), although there was a clear impact of a small number of performed measurements. Namely, the R^2 values significantly increased (by a factor of 2 or more) when data of two outlier patients were excluded from the analysis. Since fluid removal (and thus changes in hydration status) differed widely among individual patients, the weak correlation of changes in ϕ and r with the amount of the fluid removed during HD may also indicate a nonlinear pattern of the relation between ϕ, r and skin water content or between the skin water content and total body water.

The calculated values of the complex refractive index N_{ep}, measured at the volar forearms and fingertips, are shown in figure 3(a). In the graph, each vector links two measurements at the same spot, pointing from the value before HD to that after HD. For the forearms, one can see a total spread of values for the real part from 1.6 to 2.75 and from 0.4 to 1.7 for the imaginary part. However, the most distant data were obtained in a few measurements, and the bulk of the values is centred in a close vicinity of the value of $1.75 + 0.7i$. The real part is in good agreement with the value 1.7 reported for skin measured *in vitro* (Fitzgerald *et al* 2003), though the anatomical location of the skin is not stated in that work. In contrast, our values of the imaginary part κ_{ep} are in all cases somewhat higher than those reported earlier, 0.25 (Fitzgerald *et al* 2003, Siegel 2004) and 0.4 (Pickwell *et al* 2004).

The vectors corresponding to measurements on fingers are located clearly in a different portion of the complex plane, with the real part mostly higher—its mean value being close to 2—and the imaginary part lower than that at forearms. The values are markedly less scattered, and also the vectors are shorter owing to smaller differences occurring during the HD. The
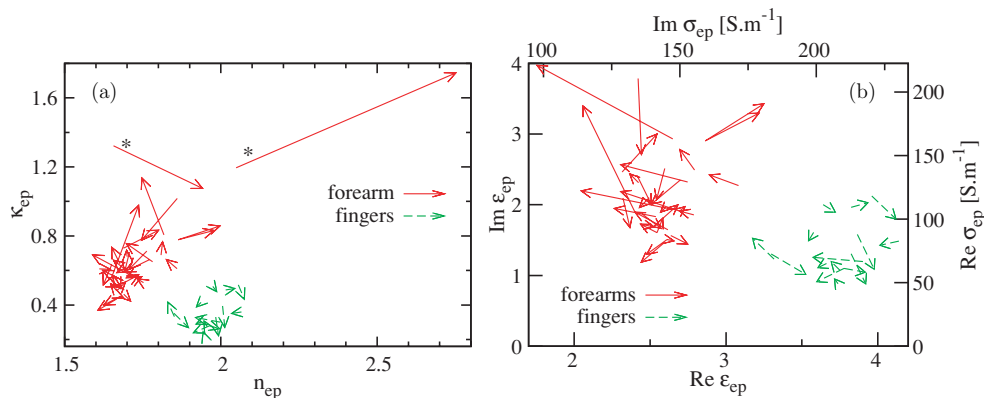
Figure 3. Vectorial representation of changes in the complex optical constants of epidermis before and after dialysis. (a) Refractive index, (b) permittivity and conductivity at 1 THz. For the sake of clarity, the scale of the right graph is chosen such that the two vectors marked by asterisks are out of range.

obtained real part is similar to the value stated in previous work (Pickwell *et al* 2004) for what is called 'normal skin' at 1 THz.

Another representation of the data, transformed to the complex permittivity and conductivity, is shown in figure 3(b). One can see that the real part of the permittivity for the forearms and fingers lies in different intervals—that of the forearms is found to range roughly from 2 to 3 and that of the fingers from 3 to 4. In contrast, the intervals found for imaginary parts overlap, spanning from 1 to 2 for fingers and from 1 to about 4 for the forearms. These values can be compared with those found indirectly using electromagnetic simulations of power reflectance R of the palm performed in the 75–110 GHz range (Feldman *et al* 2008) where the values of $\varepsilon_{ep} = 3$, $\sigma_{ep} = 0.025$ Sm^{-1} of the epidermis tissue were successfully used to compute the experimental data. In that work, the model of epidermis can be understood as a metamaterial comprising the tissue matrix and helix-like conductive structures representing sweat ducts. Their conductivity achieves values of the order of thousands of Sm^{-1} and it increases with the sweating activity. We do not expect the sweating to play a dominant role in our measurements as the patients were examined in a room with a stable temperature of $21°C$ and did not exert any physical activity. However, according to Feldman *et al* 2008, the reflectance of the skin at 0.11 THz is equal to at least $R = 0.45$ and the conductivity of the sweat ducts remains significant even in the calm state. From these findings it follows indirectly that in the lower THz range, the skin behaves as a composite medium with a negative real part of the effective permittivity. In contrast, values derived from our measurements typically do not exceed $R = 0.15$ above 0.3 THz. Therefore we suggest that the plasma frequency is located within the frequency range 0.11–0.3 THz; this would agree with the pronounced dispersion (increase of R) observed at the lower edge of our accessible spectral range.

The interpretation of the TDTS measurements, as represented by the irregular patterns displayed in figure 3, in terms of body hydration status is not clear. For this reason, we have attempted to find a relationship between changes of the refractive index during HD and the volume of fluid removed by ultrafiltration. These values corresponding to forearm measurements are shown in figure 4. One would expect that subjects from whom a low amount of fluid was removed would exhibit a small absolute value of changes in N_{ep}; however, the distribution of the symbols in the graph does not seem to follow this simple rule, and the
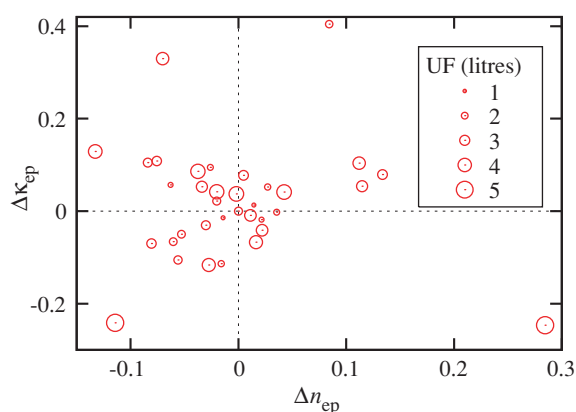
Figure 4. Changes of the complex refractive index N_{ep} at volar forearm for all patients. The size of the symbols is scaled according to the fluid volume removed by ultrafiltration (UF). For a convenient scaling, one point at $\Delta n_{ep} = 0.7$, $\Delta \kappa_{ep} = 0.55$ is omitted.

same holds for this kind of data obtained at fingertips (not shown). Here again, there is no straightforward data interpretation. The data fall into all quadrants, with only a small part of them lying in the fourth one ($\Delta n > 0$, $\Delta \kappa < 0$). There seem to be three preferential directions of change—a substantial part of the data forms a three-lobed shape centred at the coordinate origin. However, even after studying these data in relation to other measured parameters including the overhydration parameters obtained from BIS, we were not able to achieve an understanding of this result.

5. Conclusion

Using TDTS and a dedicated methodology we have performed a small-scale study, to our knowledge the first one of its kind, with the aim of determining experimentally the influence of haemodialysis on the content of water in human skin. Marked changes of the epidermis refractive index N_{ep} at the volar forearm were detected while the influence of HD on N_{ep} at the fingertips is much smaller. Also, our experiments have revealed a clear difference between the values of N_{ep} at forearms and fingers. However, the data collected in our measurements, including BIS and other patient-dependent parameters, did not allow us to elucidate the underlying mechanism which determines the THz refractive index N_{ep}. Consequently, it appears that the measured refractive index of the skin, at least at the two selected body parts, is not related directly to the body hydration status alone and at this stage of our knowledge, without further corrections or enhancement of the method, this approach cannot be employed for monitoring the progress of HD. As a further step, it would be possible to focus on other parts of the patients' skin or, alternatively, to exploit electromagnetic radiation with different frequencies in another attempt to find correlations between the skin response and overall body hydration status.

Acknowledgments

References

Dreyhaupt A, Winnerl S, Dekorsy T and Helm M 2005 High-intensity terahertz radiation from a microstructured large-area photoconductor *Appl. Phys. Lett.* **86** 121114

Fayomi O, Maconochie I and Body R 2007 Towards evidence based emergency medicine: best BETs from the Manchester Royal Infirmary. Is skin turgor reliable as a means of assessing hydration status in children? *Emerg. Med. J.* **24** 124

Feldman Y, Puzenko A, Ishai P B, Caduff A and Agranat A J 2008 Human skin as arrays of helical antennas in the millimeter and submillimeter wave range *Phys. Rev. Lett.* **100** 128102

Ferguson B and Zhang X-C 2002 Materials for terahertz science and technology *Nature Mater.* **1** 26

Fitzgerald A J, Berry E, Zinovev N N, Homer-Vanniasinkam S, Miles R E, Chamberlain J M and Smith M A 2003 Catalogue of human tissue optical properties at terahertz frequencies *J. Biol. Phys.* **129** 123

Fitzgerald A J, Wallace V P, Mercedes J L, Bobrow L, Pye R J, Purushotham A D and Arnone D D 2006 Terahertz pulsed imaging of human breast tumors *Radiology* **239** 533

Kyle U G *et al* 2004 Bioelectrical impedance analysispart: I Review of principles and methods *Clin. Nutrition* **23** 1226

Mandal A K, Baig M and Koutoubi Z 1996 Management of acute renal failure in the elderly: treatment options. *Drugs Aging* **9** 226

Matthie J, Zarowitz B, de Lorenzo A D, Andreoli A, Katzarski K, Pan G and Withers P 1998 Analytic assessment of the various bioimpedance methods used to estimate body water *J. Appl. Physiol.* **84** 1801

Nahata A, Yardley J T and Heinz T F 1999 Free-space electro-optic detection of continuous-wave terahertz radiation *Appl. Phys. Lett.* **75** 2524

Pickwell E, Cole B E, Fitzgerald A J, Pepper M and Wallace V P 2004 In vivo study of human skin using pulsed terahertz radiation *Phys. Med. Biol.* **49** 1595

Pickwell E and Wallace V P 2006 Biomedical applications of terahertz technology *J. Phys. D: Appl. Phys.* **39** R301

Siegel P H 2004 Terahertz technology in biology and medicine *IEEE Trans. Microwave Theory Tech.* **52** 2438

Vivanti A, Harvey K, Ash S and Battistutta D 2007 Clinical assessment of dehydration in older people admitted to hospital What are the strongest indicators? *Arch. Gerontol Geriatr.* (PubMed PMID 17996966)

Woodward R M, Cole B E, Wallace V P, Pye R J, Arnone D D, Linfield E H and Pepper M 2002 Terahertz pulse imaging in reflection geometry of human skin cancer and skin tissue *Phys. Med. Biol.* **47** 3853